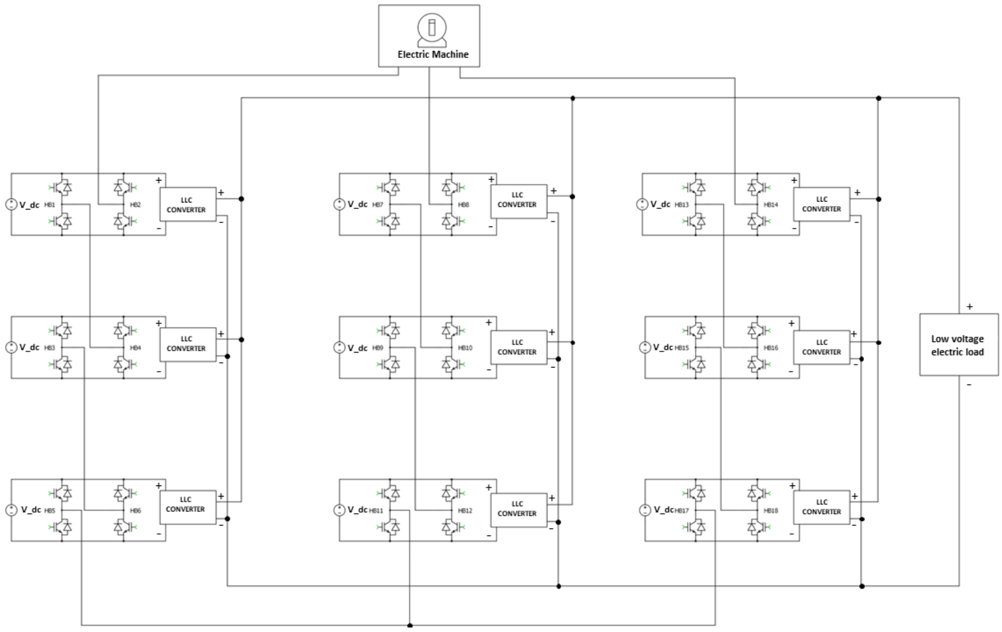

Distributed DC/DC converter system

Maintaining voltage stability and efficiency optimization while regulating several converters

Master's thesis in Electrical Engineering

MARKUS JOHANSSON
ISABELLA TEPP

DEPARTMENT OF ELECTRICAL ENGINEERING
CHALMERS UNIVERSITY OF TECHNOLOGY
Gothenburg, Sweden 2024
www.chalmers.se

MASTER'S THESIS 2024

Distributed DC/DC converter system

Maintaining voltage stability and efficiency optimization while regulating several converters

MARKUS JOHANSSON
ISABELLA TEPP

Department of Electrical Engineering
Division of Electrical Power Engineering
CHALMERS UNIVERSITY OF TECHNOLOGY
Gothenburg, Sweden 2024

Distributed DC/DC converter system
Maintaining voltage stability and efficiency optimization while regulating several converters

MARKUS JOHANSSON

ISABELLA TEPP

Supervisor: Torbjörn Larsson, Volvo Cars, Aditya Pratap Singh, Volvo Cars & Torbjörn Thiringer, Chalmers
Examiner: Torbjörn Thiringer, Department of Electrical Engineering

Master's Thesis 2024
Department of Electrical Engineering
Division of Electrical Power Engineering
Chalmers University of Technology
SE-412 96 Gothenburg
Telephone +46 31 772 1000

Cover: A multilevel converter system with LLC converters connected in parallel

Typeset in LaTeX
Printed by Chalmers Reproservice
Gothenburg, Sweden 2024

Distributed DC/DC converter system
Maintaining voltage stability and efficiency optimization while regulating several converters
MARKUS JOHANSSON, ISABELLA TEPP
Department of Electrical Engineering
Chalmers University of Technology

Abstract

This thesis is about the investigation of a new concept regarding the supply of the low voltage side in battery electrical vehicles. The concept is about supplying the low voltage side with a multilevel converter (MLC). A control strategy was tested that is based on distributing different set voltages to each converter. The system was meant to regulate itself with no other information other than the input voltage and output voltage. The system needs to fulfil the requirements of LV124. The test sequences performed showed that a system of three converters can handle power loads ranging from approximately 20−600 W, while still fulfilling the LV124 requirement. The test sequences were performed on a system of converters with different set voltages as well as with the same set voltage. The result was that the test case with converters on the same set voltage performed better regarding both the overall efficiency as well as the voltage stability. However, the theory behind this thesis and the simulated models counter this result, meaning that a system with different set voltages would improve the overall efficiency. This unpredicted result can be concluded to be the cause of a hardware that is still in the early stages. With further development of the hardware to improve efficiency and control strategy to improve voltage stability of the system, this MLC system could possibly supply the low voltage side.

Keywords: DC/DC converter, multilevel converter, battery electrical vehicle, set/target voltage

Acknowledgements

We would like to express our thanks to our examinor Professor Torjörn Thiringer for his insightful ideas and guidance throughout this project. We are also deeply grateful for our other Torbjörn, Torbjörn Larsson, who designed this thesis for us and has been with us throughout the entire journey, steering us in the right path and providing us with the technical knowledge and support necessary for the completion of this work.

Additionally, we would like to extend out gratitude towards Aditya Singh who has been immensely helpful every time we encountered obstacles. His patience and assistance have been crucial to our progress.

And lastly, a large thank you to Jonas Forssell and everyone at Volvo Cars who has helped us and been a part of this project. We have felt incredibly included and supported and it has been a pleasure being part of this team.

Markus Johansson & Isabella Tepp, Gothenburg, June 2024

List of Acronyms

Below is the list of acronyms that have been used throughout this thesis listed in alphabetical order:

AC	Alternating current
BEV	Battery Electrical Vehicle
BMS	Battery Monitoring System
DC/DC	Direct current to direct current
DTOC	Definite time overcurrent
EMI	Electromagnetic interference
LV	Low voltage
MLC	Multilevel converter
PCB	Printed circuit board
PFM	Pulse frequency modulation
PWM	Pulse width modulation
SOC	State of charge
WLTP	Worldwide Harmonised Light Vehicles Test Procedure
ZCS	Zero current switching
ZVS	Zero voltage switching

Contents

List of Acronyms **ix**

1 Introduction **1**
1.1 Ethics and sustainability 1
1.2 Problem background 1
1.3 Purpose 3
1.4 Limitations 3

2 Theory **4**
2.1 DC/DC converter 4
2.1.1 Topology 4
2.1.2 Resonance and switching frequency 5
2.1.3 Regulator of the DC/DC converter 6
2.2 Modeling theory 8
2.2.1 Transformer model 8
2.2.2 Core loss calculation 9

3 Case setup **10**
3.1 System level 10
3.2 DC/DC converter 11
3.2.1 Control strategy for all DC/DC converters 13
3.3 QSPICE − Simulating losses 14
3.4 PLECS − DC/DC converter model 15
3.4.1 Single DC/DC converter model 15
3.4.2 Multiple DC/DC converters in parallel 16
3.5 Hardware test setup 18
3.5.1 Hardware analysis 18
3.5.2 Battery module testing 19
3.5.3 Software implementations 21

4 Results and analysis **22**
4.1 Load switching sequences 22
4.1.1 One DC/DC converter 22

4.1.2 Multiple DC/DC converters 24
4.2 Overheating function 29
4.3 Multiple DC/DC converters handling WLTP cycle 30
4.4 Efficiency 32
4.4.1 Test sequence 35

5 Conclusion **38**
5.1 Future work 39

Bibliography **41**

1

Introduction

The electric vehicle has risen in popularity in the last years as a sustainable transportation and the industry have now shifted its focus from the internal combustion engine (ICE) propulsion to electric drives. To further improve the efficiency of electric vehicles it is necessary to develop new concepts and techniques for the low voltage side.

In a combustion vehicle, the low voltage side is driven by a battery and a generator which is powered by the combustion engine. An electric vehicle uses the same system but with power electronic conversion from the high voltage battery instead of the generator. Thus, it is of interest to develop a system with several DC/DC converters to enhance the operating range of the converter to further increase the efficiency of the system.

1.1 Ethics and sustainability

The change from the ICE to electric drives can reduce greenhouse gas emissions and contribute to a sustainable development as the transport sector is a large contributor to greenhouse gas emissions. The global electric vehicle fleet is estimated to grow from 2022 to 2030, increasing the electricity consumed by electric vehicles from 110 TWh to 950 TWh. The global electricity production in 2019 was composed of 63 % fossil fuels, 10.3 % nuclear energy and 29.1 % renewable sources [1]. The global emission from generation of electricity is estimated to be 420 g CO_2e/kWh in 2024 [2]. Therefore it is of great interest to look at new solutions for increasing energy efficiency in the vehicle.

An electric vehicle has zero tailpipe emissions which will lower air pollutants such as nitrogen oxides (NOx) and particulate matter (PM). Reducing pollution from vehicles can foster healthier ecosystems, the benefits range from improved agricultural and enhanced biodiversity, which both play a crucial role in providing essential resources to the human population. Moreover, the batteries and electric motors requires a large amount of resources. By minimizing the use of these materials, there can be a decrease of the environmental impact.

1.2 Problem background

Today's battery electric vehicles (BEVs) are constructed with a DC/DC converter between the high and low voltage (LV) side which feeds the low voltage side. The low voltage side consists of a 12 V battery working in parallel with the converter to support loads on the low voltage side. The 12 V load is highly dynamic causing the converter to operate in a broad range. The window where the converter has the best efficiency is therefore only a small region in the operating range, reducing the overall efficiency.

The converter is an important component in the vehicle and a fault in this component can make the vehicle non-functioning. Therefore it is of interest in the automotive industry to investigate other methods on how to supply the low voltage side of the vehicle to increase efficiency and robustness.

This thesis is about exploring the idea of a new system for the low voltage side without the 12 V battery and simultaneously dividing the DC/DC converter into several small DC/DC converters. The task is to investigate if the low voltage side can be supplied by a multilevel converter (MLC) [3].

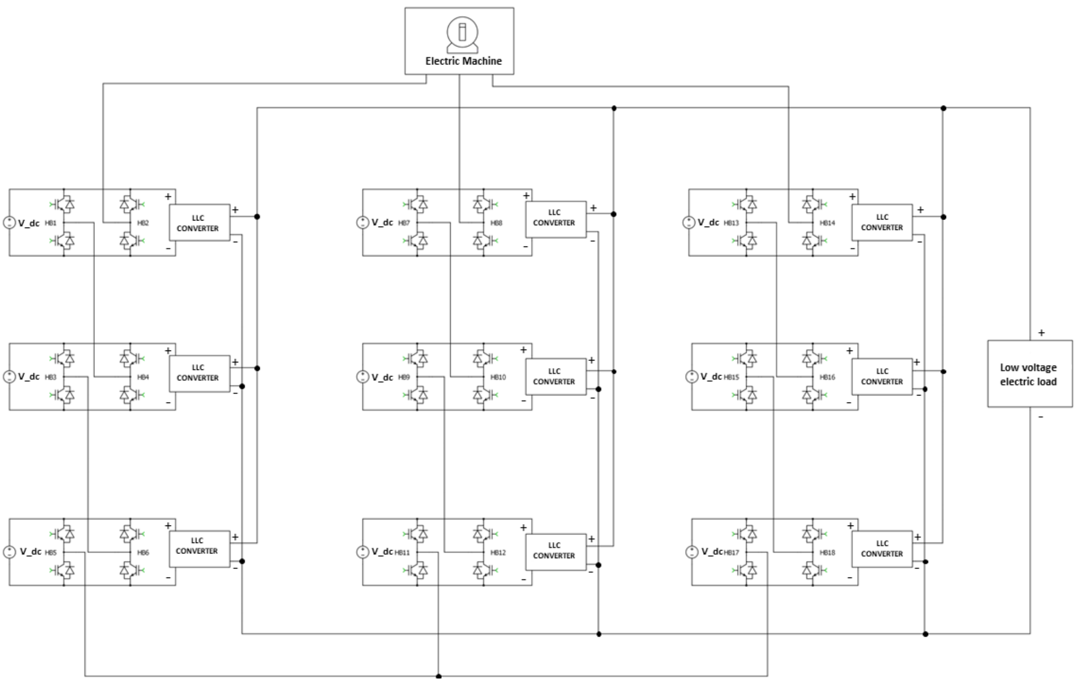

Figure 1.1: Topology of a multilevel converter with DC/DC connected to each leg

The removal of the 12 V battery can possibly contribute to an overall cost- and weight reduction since it is both expensive and heavy. Theoretically and hopefully, this could result in a lighter system with higher efficiency since the operating range of the DC/DC converters can be optimized to be working at the most efficient operating point. The robustness of the system will also be strengthened as the functionality of the system will be divided between several DC/DC converters instead of only one. The system will utilize the possibility of having the minimum number of DC/DC converters active at lower loads to increase efficiency. From this follows the requirement that the system needs to react fast enough to handle the unpredictable changes in the load without the 12 V battery as backup.

The system will be controlled by a master control unit that will determine which DC/DC converter that should operate depending on the high voltage battery's state of charge (SOC) and the predictable load changes. With several DC/DC converters there will be a lot of cable harness for communication, therefore it is also interesting to evaluate if communication should be done by wire or radio.

1.3 Purpose

The purpose of this thesis is to investigate and model a DC/DC converter system with a high efficiency which is able to supply the vehicle with the needed LV electrical system power. Within this purpose some goals were:

- To model a DC/DC system that would fulfil requirement LV124 which specifies that the low voltage system of the car needs to be within $9 - 16\,\mathrm{V}$ while driving
- The DC/DC system should be able to handle load transients without too large voltage dips
- To distribute the set voltages in a way such as to achieve the highest efficiency

Example of current transients that could occur are turning the wheel, pressing the brake pedal and maximum coupe heating. The system also needs to be redundant, if several DC/DC converters break down, the vehicle should still be able to operate in a safe manner.

1.4 Limitations

One of the limitations of this thesis report is that design of the prototype DC/DC converter is not changeable when it comes to the hardware, the aim is to optimize how the converters are used. For the thermal losses of the system, no investigation will be considered.

2
Theory

The following chapter will delve into the theory behind the DC/DC converter, which is the main component of this master thesis. Basically, the DC/DC converter is a component that transforms one DC input voltage level into a different DC output voltage level. This conversion can be done in many ways, each tailored to different purposes when it comes to efficiency, size and cost.The main objective of the concept is to obtain high efficiency, with a galvanic separation that ensures that the system cannot take damage if there is a fault up or downstream of the DC/DC converter. Because of this, and its suitability for low power applications [4], the LLC resonant converter has been chosen to study as a DC/DC converter.

2.1 DC/DC converter

The input voltage to the converter is dependant on the battery voltage/state of charge (SOC) so it operates with varying input voltage. The electrical LV load in a car is dynamic, there can in fact also be substantial transients, for example, if the brake pedal is pressed and the steering wheel is turned at the same time. The properties of the LLC topology fits this environment as it can soft-switch throughout the whole operating region and obtain high efficiency even with a varying input voltage and dynamic electrical LV load. LLC converters also have a low electromagnetic interference (EMI) [5], which is suitable for vehicle application.

2.1.1 Topology

The topology of the DC/DC converter for this thesis is chosen to be a half-bridge LLC resonant converter, which is able to boost or lower the incoming voltage to the desired output voltage. The converter is made up of four different blocks; power switches, resonant tank, transformer and a rectifier [6]. Both the power switches and the rectifier block use MOSFETs with different gate-driven circuits to achieve the desired output.

The power switch block is a half-bridge which uses unipolar switching to obtain a square wave pulse with a DC-offset by $V_{in}/2$. Deadtime is needed between the switching to prevent simultaneous conduction of two transistors in a phase leg and also to allow time for zero voltage switching (ZVS). The switching is controlled by a gate-driver which uses pulse frequency modulation (PFM) with a fixed duty cycle of 0.5.

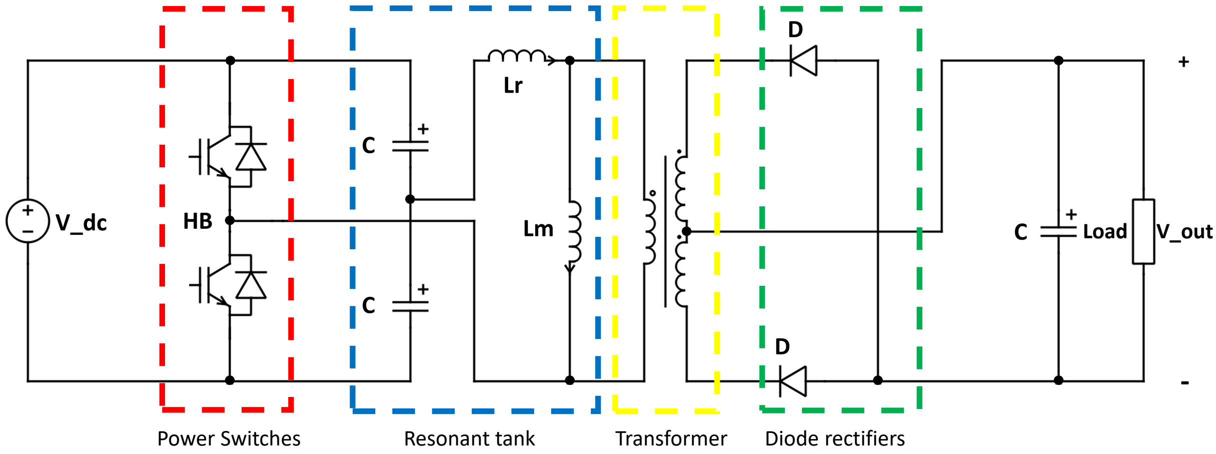

Figure 2.1: Circuit schematic of a simplified LLC converter

The resonant tank consists of a capacitance, C_r and an inductance which is split into a series resonant inductance, L_r, and the transformers magnetizing inductance, L_m. The current circulates in the resonant tank and is delivered to the load via the transformer. When the frequency changes, the behaviour of the resonant tank will change as the impedance of the capacitor and inductor are dependent on the frequency. Operating close to the resonance frequency will yield lower losses in the converter as the impedance of the resonant circuit is low at this point. Resonance frequency is a critical factor for the converter's operation and design.

The rectifier tank on the secondary side of the transformers consists of two MOSFETs which acts like a diode without forward voltage drop. The mosfets will rectify the square wave to a DC output which will be filtered by an output capacitor to smoothen the output.

2.1.2 Resonance and switching frequency

As stated earlier, operating close to the resonance frequency of the circuit will minimize the losses and maximize the efficiency [4]. The resonance frequency for the circuit can be calculated by solving the equation for when the impedance generated by the inductors and capacitors in the resonant tank, see Figure 2.1, cancel out each other, i.e. solving the equation

$$Z_C + Z_L = 0 \implies \frac{1}{j\omega C} + j\omega L = 0 \implies \frac{1}{\sqrt{CL}} = \omega = 2\pi f \tag{2.1}$$

where Z_C and Z_L are the impedance of the capacitor and inductor, C is the capacitance, L is the inductance, ω is the angular velocity in radians and f is the frequency in Hz.

The resonance frequency of the LLC circuit can then be written as [7]

$$f_0 = \frac{1}{2\pi\sqrt{C_r L_r}} \tag{2.2}$$

Having the mosfets operating at a switching frequency equal to the resonance frequency would be ideal, but since there is only a single resonance frequency point and the input and output of the system can vary, the switching frequency can have a broad range. Obtaining zero current switching (ZCS) and a smooth commutation of the rectifier diodes on the secondary side is still possible even if not operating precisely at resonance frequency. To obtain ZCS while having a switching frequency above or below the resonance frequency, the losses of the system will increase [8]. Figure 2.2 presents how the different currents and voltages of the system behave depending on whether resonance frequency is achieved or not. The figure shows the voltage over the two MOSFET gates, V_{g_Q1} and V_{g_Q2}, the currents through the primary side (I_r), through the transformer (I_m) and through the diodes on the secondary side (I_s).

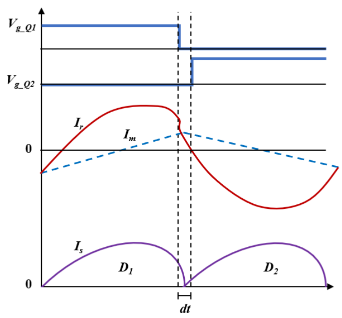

(a) Behaviour above f_0

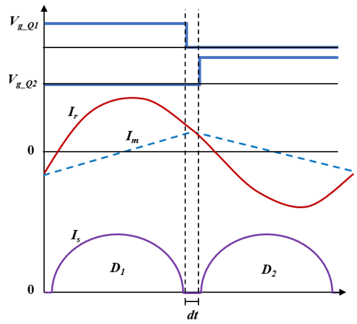

(b) Behaviour at f_0

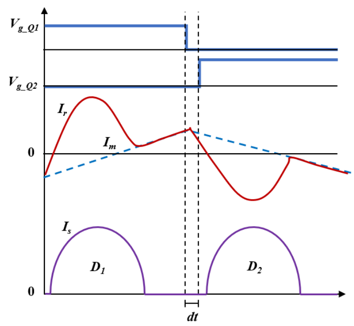

(c) Behaviour below f_0

Figure 2.2: Plots of the voltage and current through the converter for different frequencies

2.1.3 Regulator of the DC/DC converter

The task of the DC/DC converter is to either boost or lower the voltage. The way an LLC resonant converter does this is through the operating frequency of the system. The control of the regulation is done through a PID controller. A PID control loop uses proportional gain (K_p), integral (K_i) and derivative (K_d) influence on the controller output. The desired signal $r(t)$ is compared to the output signal $u(t)$ to get an error value $e(t) = r(t) - u(t)$. The error value is then put through the PID steps and the new output function can be calculated as

$$u(t) = K_p e(t) + K_i \int_0^t e(t) + K_d \frac{de(t)}{dt} \tag{2.3}$$

For the DC/DC converter, the desired signal $r(t)$ is the set voltage. Figure 2.3 shows a flowchart of the PID controller.

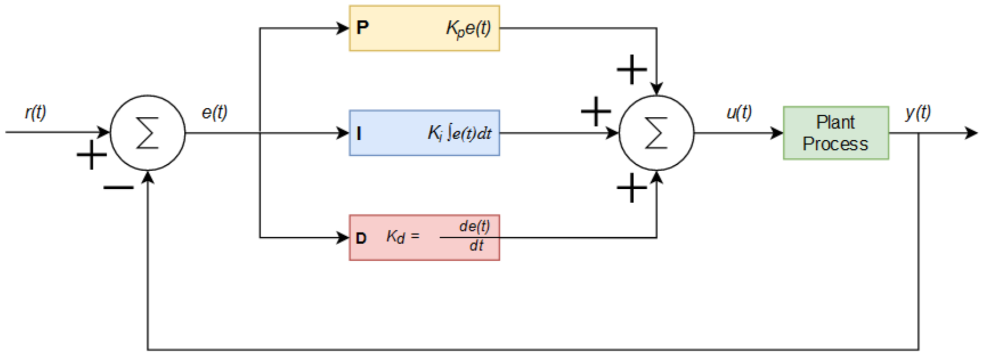

Figure 2.3: Standard PID-regulator flowchart

Depending on the voltage gain of the system, the DC/DC converter will regulate itself to a certain frequency. A typical gain curve looks as Figure 2.4. The voltage gain is defined as the output voltage over the input voltage and the normalized frequency is compared with the self-resonance frequency.

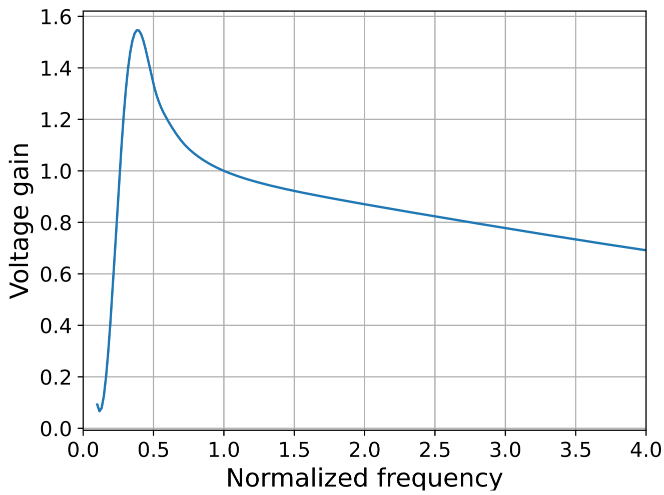

Figure 2.4: Gain curve plotted against the normalized frequency

In the graph above, it is clear that for a stronger gain in voltage, lower frequency is needed and for a smaller gain, higher frequency is needed. A risky region is below the frequency at peak gain. In the region, going to the left hand side of the peak is harder to control through the frequency due to its steep slope. Going to far in the other way is not efficient either since the higher the frequency the larger the switching losses. Taking this into account the converter needs to be limited both from below and above in frequency [9].

2.2 Modeling theory

Since simulations are not perfectly representing the real world some additions often needs to be done. Modeling the converter exactly as the hardware is constructed will not yield the proper behaviours of the hardware, therefore some alterations has been done.

2.2.1 Transformer model

Texas Instrument stated in [10] that the model of an LLC resonant converter cannot be done exactly according to its theory. Specifically, the resonance tank. To model a more realistic resonance tank the values of the inductances need to be modified. In a regular model for an LLC, displayed in Figure 2.5, there are C_r, L_r and L_m included in the resonance tank, outlined in red.

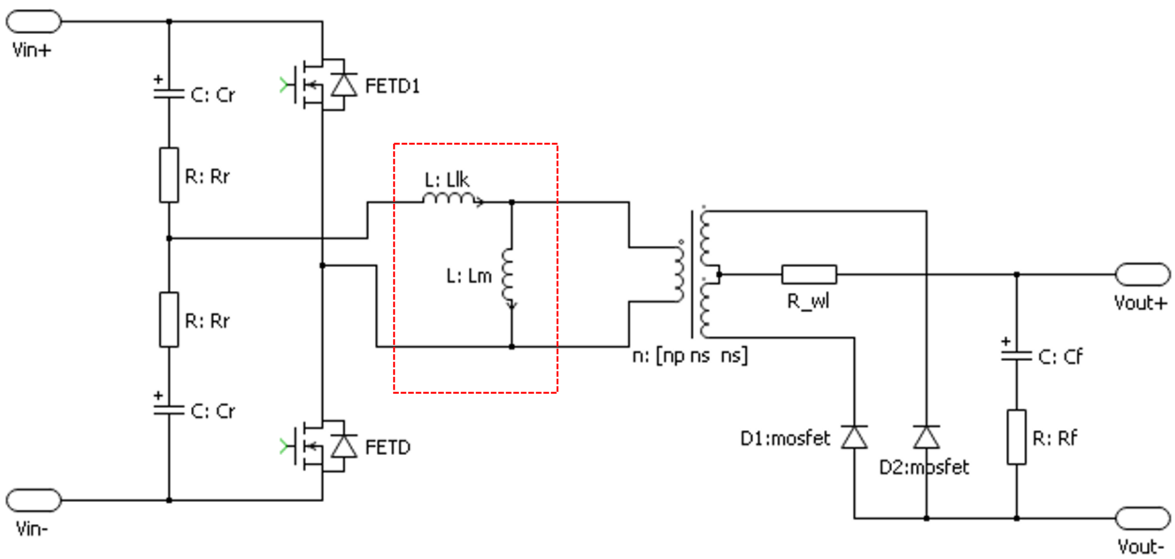

Figure 2.5: Model of a regular LLC converter

According to [10], a more accurate model can be built as in Figure 2.6, where the inductive part of the tank now consists of three inductors.

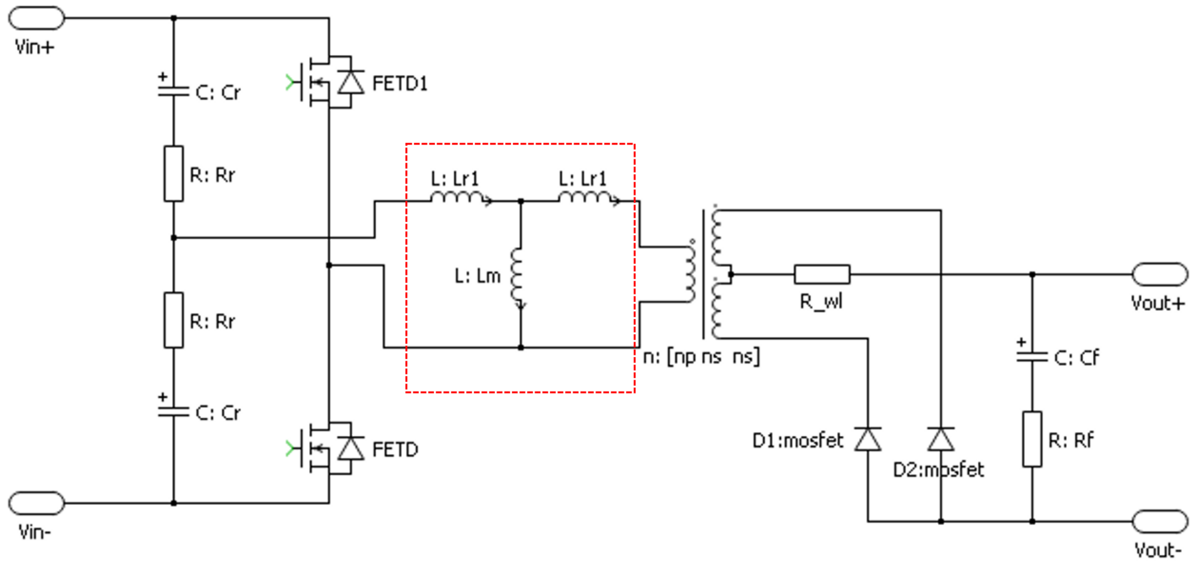

Figure 2.6: A modified model of an LLC converter

In the modified model above, the new components L_{r1} and L_m can be calculated as [10]

$$L_m = kL_p \tag{2.4}$$

$$L_{r1} = (1-k)L_p \tag{2.5}$$

$$k = \sqrt{1 - \frac{L_{lk}}{L_p}} \tag{2.6}$$

where L_{lk} is the leakage inductance, L_p the primary inductance when the windings are open and k is a relation constant between the two inductances.

2.2.2 Core loss calculation

The simulation conditions are always ideal, so including things such as losses often needs to be done externally. The transformer core has huge impact on the losses of the DC/DC converter. The method for estimating this has been chosen to Steinmetz's method. Steinmetz's equation is an empirical equation used to calculate the core losses in magnetic materials that are subjected to external sinusoidally varying magnetic flux [11]. The equation follows below

$$P_v = k \cdot f^a \cdot B^b \tag{2.7}$$

where P_v is the average power loss per unit volume in mW per cubic centimeter, f is the frequency in kHz and B is the peak magnetic flux density in mT. The coefficients k, a and b are the Steinmetz coefficients which are parameters that can be extracted from material documentation.

3

Case setup

The main objective of this project is to model a realistic DC/DC converter system in an appropriate simulation environment. After a model had been constructed, it had to be converted into a C-script to run the system in a test rig. The test rig that was tested on consists of three clusters with one DC/DC on each cluster, where each cluster contains four battery cells. This chapter has a purpose to explain this entire process and what was done to optimize the system.

Some specifications for values such as the range of input and output voltage, maximum power from one DC/DC converter, electrical LV load in a car, example of electrical load transients and the number of cells in the test rig follows in Table 3.1.

Table 3.1: Specifications for the system of DC/DC converters

Parameter	Value
V_{in}	$13.3 - 16.8$ V
V_{out}	$13.5 - 15.5$ V
P_{max}/DC/DC	200 W
Number of cells	12
P_{car}	$10 - 6000$ W
$P_{transient}$	1500 W

A total power of approximately $6000/200 = 30$ DC/DC converters would then be required to supply a car, but since that would consume too much computational power, the model of multiple DC/DC converters has been reduced down to three. Maximum power loads have then been scaled down to suit the modeled DC/DC system.

3.1 System level

The system consist of a high voltage battery, masterboard, DC/DC converters and the low voltage load. The battery feeds the DC/DC converter with energy and the battery monitoring system (BMS) updates the masterboard about the SOC. The masterboard communicates with the DC/DC converter by a radio protocol.

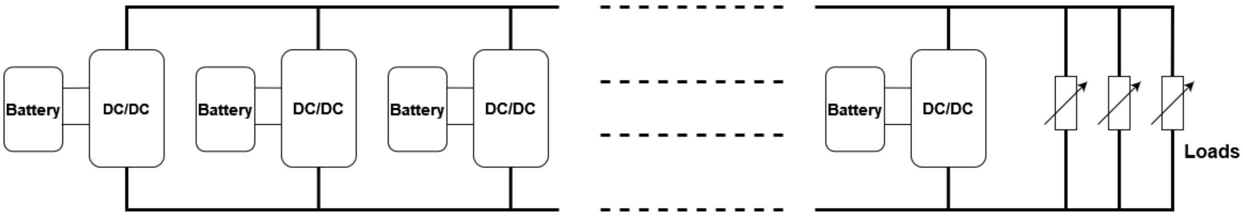

Figure 3.1: Block diagram of the low voltage system. DC/DC converters are connected in parallel with the electronic load

The DC/DC converter regulates itself to the set voltage, through a PID controller. The set voltage is given by the masterboard and the DC/DC converter will react instantaneously when the load changes.

3.2 DC/DC converter

Figure 3.2 below displays the schematic of the half-bridge LLC. The input to the DC/DC converter is to the left followed by a capacitance bank, split into two C_r and two MOSFETs. The resonance bank consists of two inductors, leakage inductance L_{lk} and magnetizing inductance L_m. The ratio between the windings on the primary and secondary side is 1 : 2 : 2. On the secondary side of the converter two diodes without forward voltage drop are placed, representing the synchronous switching MOSFETs. The voltage from the secondary side is compared with the set voltage of the DC/DC converter and goes through a PID controller that calculates what frequency the MOSFETs on the primary side should operate at.

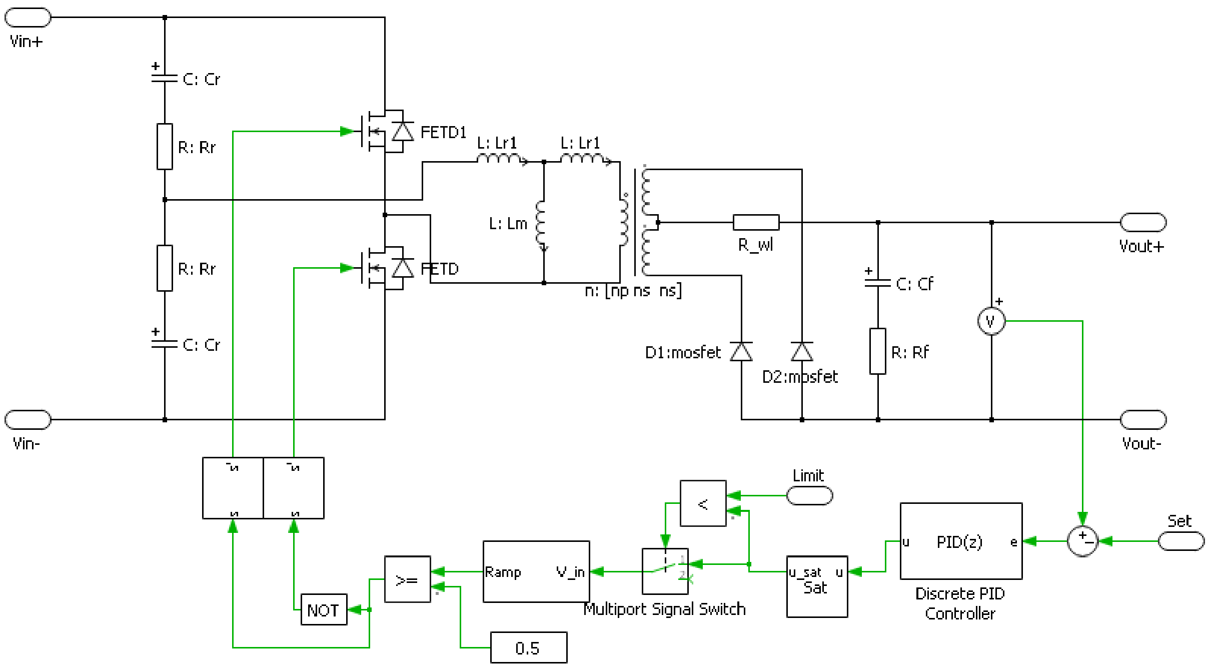

Figure 3.2: Schematics inside of the LLC converter

Below in Table 3.2 the values for parameters in Figure 3.2 are presented. The values are taken from the hardware and used in the PLECS model.

Table 3.2: Parameters used in the PLECS model

Parameter	Value
C_r	13.2 μF
L_{lk}	84 nH
L_m	670 nH
L_{r1}	43 nH
n_p	1
n_s	2
U_{lim}	500 kHz
$Llim$	75 kHz

The resonance bank of the converter consists of 2 C_r capacitors. The variables L_m and L_{r1} were retrieved by following (2.4)-(2.6). The hardware has a power limit of 200 W which is needed to be accounted for in PLECS.

The converter takes in values for the set voltage. Depending on whether the input voltage from the battery cells is lower or higher than the set voltage, the frequency of the converter will increase of decrease. Using the difference between the input voltage and set voltage, the PI controller in the converter outputs the frequency the MOSFETs should operate at. The frequency needs to be limited, as explained in 2.1.3. The upper and lower saturation limit for the PI is set to 75 and 500 kHz respectively.

The DC/DC converter is controlled by the frequency of the half-bridge transistors which will change depending on the difference between the output voltage and the set point voltage of the DC/DC converter. The modulator in PLECS is made up by a PI-controller which will then change the frequency of the DC/DC converter. Changing the frequency will alter the impedance in the resonant tank, therefore increasing or decreasing the output voltage of the DC/DC. The PI-controller reads the output voltage and converts it into a physical value by an AD-converter in the C-script in the software. The code will update the frequency each cycle to match the desired set voltage on the output. The desired set voltage is accomplished by the PI-controller which sends the signal to the gate driver which further sends the signal to the primary sides MOSFETs with a delay between the upper and lower transistor in each DC/DC “phase leg”, to avoid shoot-through between the two MOSFETs.

The same principle is used on the secondary side to drive two MOSFETs, but instead of only using one gate driver, two are used instead. This principle is called synchronous switching and in this case the MOSFETs will act like diodes but without the diode forward voltage drop.

The output voltage needs to be limited to avoid high voltage damage to the DC/DC converter. When the output voltage is above the limit, the DC/DC converter will be shut down to avoid physical damage to itself and other components connected to the 12 V bus.

The temperature is measured via a thermistor next to the primary side MOSFETs. The DC/DC converter will also shut down whenever the temperature rises above the maximum limit.

The current is also monitored before executing the next sequence, this is done by two external components which handles the reading of the current on the primary and secondary side. This is to protect the DC/DC converter from over-currents and to protect the physical components of it.

3.2.1 Control strategy for all DC/DC converters

The control method explored in this thesis is to control the system by having several converters set at different set voltages, in such a way that the system will regulate itself and only need feedback from the masterboard for SOC level and predictable changes in load. The SOC level is reported to the masterboard where a priority list of the highest SOC levels is made. The DC/DC converters connected to the battery cells with the highest SOC should reasonably be the ones with highest set voltage.

The output voltage for the LV side of the car is preferably maintained between $13.5 - 15.5$ V, resulting in the set voltages only varying within this range. The loads on the 12 V side can be from 10 W to 7000 W. Normal driving usually consumes $20 - 30$ A which could require 2-3 DC/DC converters activated. This is where the majority of the energy is consumed and therefore this is where maximizing the efficiency and voltage stability of the system is the most important.

The main idea is to have the DC/DC converters at different set voltages so when the load changes and the voltage drops, the DC/DC converters next in line will activate. An example of the number of DC/DC converters that should be active depending on output voltage is shown in Figure 3.3.

For example when the system should maintain 15.5 V out, the total number of active DC/DC converters should be three, i.e. three DC/DC converters has set voltage of 15.5 V. If the load increases, eventually the output voltage will drop and when it has decreased to 15.0 the next six DC/DC converter with 15.0 set voltage should kick in so nine DC/DC converters in total are active, and so on. The last step of the hierarchy is to activate all of them, which will protect the system from too large voltage drops. This is also a safety measure for malfunctions.

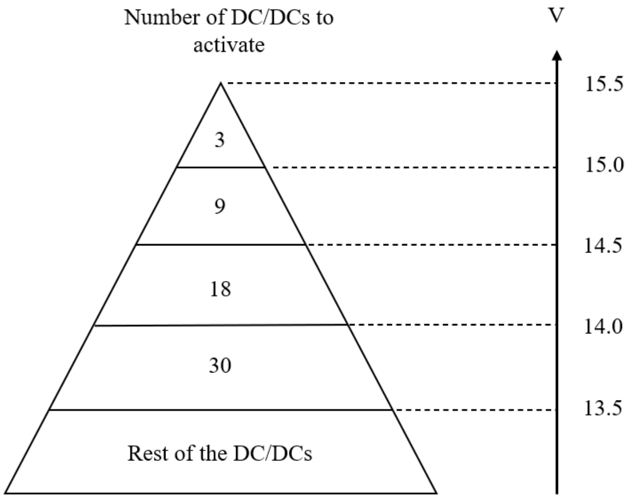

Figure 3.3: Example of a control hiearchy for the DC/DC converters and the number of them that should be activated depending on the output voltage

Most of the LV load changes in a car are unpredictable, e.g. braking. However, some LV electrical loads can send information about future changes in the load, e.g. the driver puts on the seat heater. For this new concept, an extra feature that can be done is to prepare the system for these foreseeable LV electrical load changes. As it is not a critical load like brakes, the heater signal can be delayed until the system is in a manageable condition (typically a two second delay). Depending on the size of the LV electrical load change, the masterboard will send out a request to increase the set voltage of a number of DC/DC converters. Instead of the output voltage dropping down to the last step of the hierarchy in Figure 3.3, the output voltage can stay at a higher level.

3.3 QSPICE – Simulating losses

In QSPICE a model of a single DC/DC converter, LLC half-bridge, has been implemented. QSPICE was used to calculate the losses of the converters such as, switching losses and core losses.

The loss when one MOSFET was turned on/off could be plotted and calculated to be used in a look-up table later on. The energy loss was calculated by integrating the area under the power curve. This was performed for varying voltages into the system as well as for varying currents through the MOSFETs. Measurement points were done for 12 and 16.8 V combined with currents of 12, 13, 14, 15 and 16 A. The range was determined to be this because drained cells would produce 12 V whereas fully loaded would be 16.8 V and for a maximum power of 200 W per DC/DC converter the current would range from a minimum of 12 to a maximum of 16 A.

Furthermore, there are losses in the core of the transformer that can be modelled in QSPICE. These losses were noted as well, to be used later on in PLECS via a look-up table since PLECS could not compute the core loss by itself. The calculation for core losses was done according to Steinmetz's equation (2.7).

3.4 PLECS – DC/DC converter model

The modeling of the entire system was done in PLECS. The simulated core losses from QSPICE were used in PLECS. The switching losses were implemented through a look-up table included in the Thermal Library in PLECS whereas the core losses where implemented as a resistance on the secondary side of the converter.

At first a model of a single DC/DC converter was implemented in PLECS and once that model was working as desired, multiple DC/DC converters could be connected in parallel.

3.4.1 Single DC/DC converter model

All the component values were included in the PLECS model so one DC/DC converter could be studied. Since the hardware has a power limit of 200 W the PLECS model needed to have that restriction as well. When the DC/DC converter was commanded to output more power than 200 the lower frequency limit for the MOSFETs are then raised to a suitable value so the output power saturated at 200 W.

The schematic for the model in PLECS can be seen in Figure 3.4, it shows the overview of the system with one DC/DC. In the model, calculations for core losses of the half-bridge LLC are being displayed. A voltage source, V_{in} is connected to the DC/DC converter (half-bridge LLC) which in turn is connected to a load, R_{load}. The DC/DC converter has input values for the set voltage (15.5 V in this case). The input voltage and current as well as the output voltage, current and power are probed and the calculation for the efficiency is done by

$$\eta = \frac{V_{out} I_{out}}{V_{in} I_{in}} \tag{3.1}$$

At the top of the schematic is a look-up table for the core losses (R_{loss}) of the half-bridge LLC.

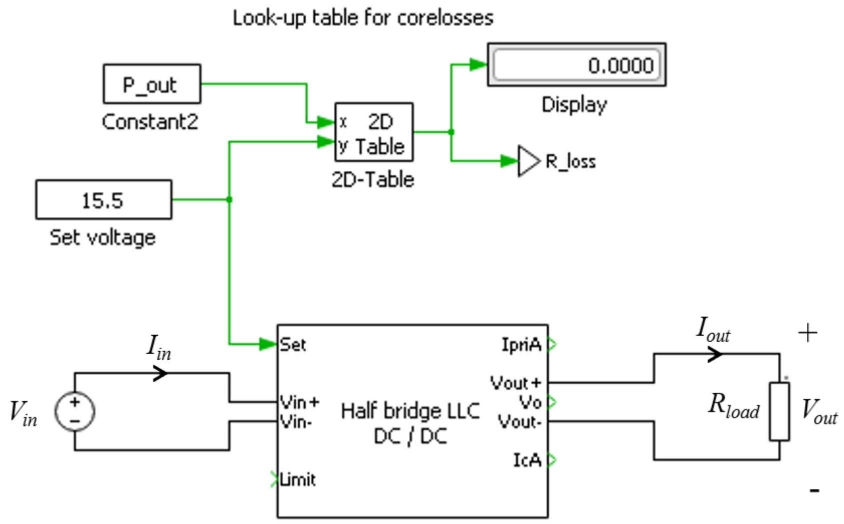

Figure 3.4: Model of one single converter in PLECS

Efficiency measurements were made in PLECS with the same measurement points as done with the hardware.

3.4.2 Multiple DC/DC converters in parallel

A system with three DC/DC converters of different set voltages was implemented. Simulations were performed for different loads to make sure that the DC/DC converter system was working as expected, i.e. that when the load was higher than the power limit of one DC/DC converter the output voltage should drop and the next DC/DC converter in line would kick in. To simulate this behaviour, which could not be attained in the simulation program alone, a C-script was implemented to check the output voltage and manually turn on or off the next DC/DC converter in line.

Simulations from one single DC/DC converter indicated that for maintaining 15.5 V out, the efficiency was highest when the DC/DC converter was operating at max load, i.e. close to 200 W per DC/DC. Therefore the 2-3 DC/DC converters that would be used the most should have the highest set voltages 15.5 V, followed by a larger group of DC/DC converters with a lower set voltage and finally the majority of the DC/DC converters at the lowest set voltage 13.5 V, as demonstrated earlier in Figure 3.3.

For simplicity and a more efficient simulation, the system with three DC/DC converters in parallel all had the same input voltage. The calculation for the core losses and efficiency were neglected in the model with multiple DC/DC converters since that requires more computational power. For the simulation to run smoothly only the necessities were included such as restraining the power output from each DC/DC converter and a C-script for turning on/off each DC/DC converter if the output voltage was below/above its set voltage. The system can be seen in Figure 3.5. Limiting the DC/DC converter to

200 W power output was done by collecting data for what frequency the DC/DC converter needed to operate at, depending on the load and voltage gain of the system. This was implemented in the system through a look-up table for the value of the lower frequency limit. On the output side of the system there is an inductor representing the inductance of the wires and a capacitor for filtering the output. A variable resistor is working as the load of the system and gets its resistance value from $R = \frac{V^2}{P}$, where P is the power from a Worldwide Harmonised Light Vehicles Test Procedure (WLTP) cycle and V is set as a constant of 15.5 V. The WLTP cycle was provided by Volvo cars and measured the total LV electrical load and voltage of a car during the test run. The C-script block contains code which regulates whether the DC/DC converters should be turned on or off depending on the output voltage. The calculation and look-up table for limiting the DC/DC converters power output are at the top.

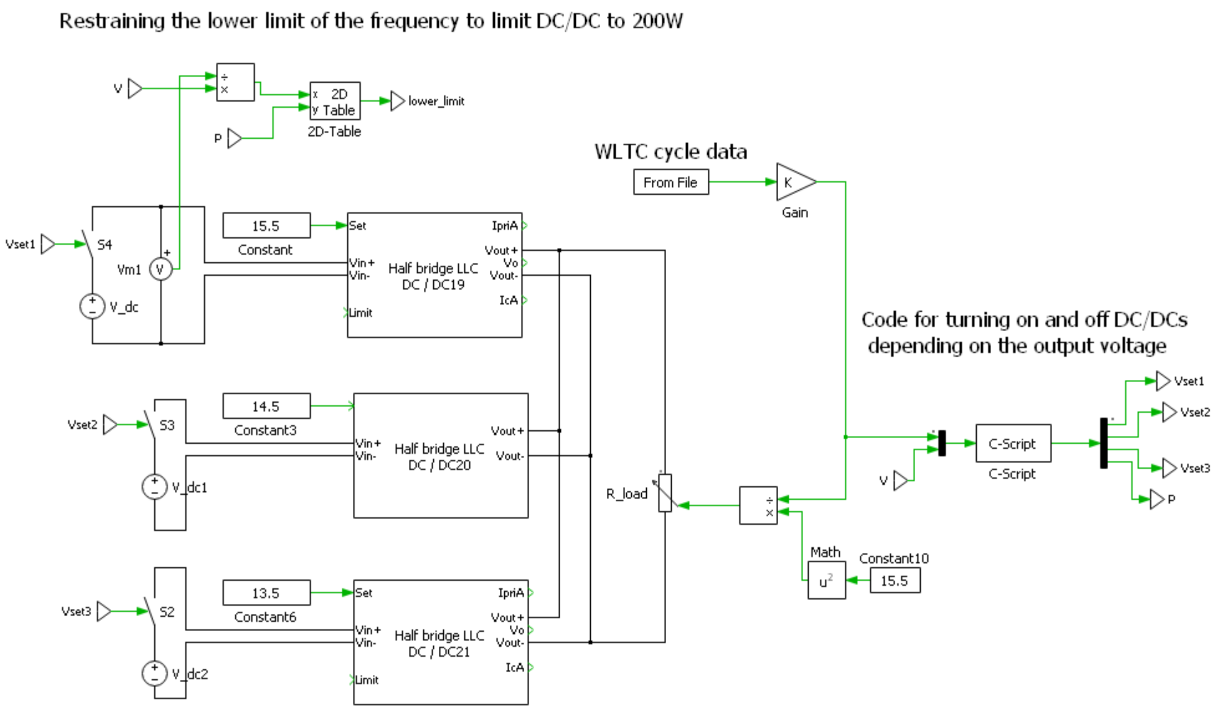

Figure 3.5: PLECS model of three DC/DC converters connected in parallel

The three DC/DC converters were set at different set voltages; 15.5, 14.5 and 13.5 V. A WLTP cycle was used as input for the load. Since the system of three DC/DC converters does not represent an entire car, the load was re-scaled to the maximum capacity of the three DC/DC converters, i.e. maximum load around 600 W. A modified WLTP cycle with extremely large transients was also used as a load to study how the DC/DC converters would respond.

Another feature that was added to the PLECS model was the ability to warn the system ahead of a large load change. This was supposed to simulate pressing the button for seat heater for example, a load which is not critical to act on instantly. When the warning of a future transient came the system should change all the DC/DC converters' set voltage to the highest, 15.5 V. This was implemented in the C-script block where the other controls for the DC/DC converter systems are done.

3.5 Hardware test setup

Testing of the DC/DC converter was first carried out with an AC/DC power supply (CPX400SP 420 W DC) and a programmable DC-electronic load (RND 320-KEL103 300W), they are displayed in Figure 3.6. Software improvements were tested out with this setup before they were tried out with the battery module since the DC supply has preventive functions for the current and voltage if they go above the set limits.

Figure 3.6: Test setup with AC/DC power supply and programmable electronic load, as well as a DC/DC converter in the middle

3.5.1 Hardware analysis

For the simulation of the DC/DC converter system to be as accurate as possible, the first thing needed was information about the actual hardware. Values for components and coded parameters of the hardware were listed in Table 3.2 previously. These parameters were used in PLECS and QSPICE to simulate a DC/DC converter that behaved similar to the hardware.

These parameters combined with the software configuration of the control board give rise to different features such as the deadtime between switches and self resonance. The latter parameters were also measured to make sure the models in QSPICE and PLECS were providing the right behaviour of the DC/DC.

For the measurement of the deadtime, the cluster board for the 15 V DC/DC converter was connected to the DC power supply. To activate the DC/DC converter, a master board was needed. With the master board connected to a computer, the code for activating the DC/DC converter could be triggered in the Segger Microcontroller Systems. Measurements were taken over both the upper and lower MOSFETs of the converter using a PicoScope® 3425. The time between the turn off signal of one MOSFET and the turn on singal of the other was measured to $24-27$ ns.

The resonance frequency of the system could be extracted when the input voltage was equivalent to the output. Probing the signals from the gate driver on the control board and measuring the frequency of the switching the self resonance was determined to be 96.4 kHz. The circuit board has a capacitance bank of 26.4 μF and leakage inductance of $L_{llk} = 84$ nH, which according to (2.2) would lead to a self resonance at 106.9 kHz.

To be able to compare the hardware and the models it was also useful to calculate the efficiency of the control board. For the measurements of the current and voltage, voltage probes were connected to the PicoScope and FLUKE *i310s* AC/DC current clamps were used to measure the current with an accuracy of ±1 % of reading ±50 A. The input and output power could then be calculated in the PicoScope and the efficiency was calculated for different scenarios, i.e. different input and set voltages combined with varying loads. The PicoScope had an accuracy of ±1 % resulting in the accumulated uncertainty of the efficiency measurements being

$$\text{Total accuracy} = \sqrt{(1\,\%)^2 + (1\,\%)^2} = \sqrt{(0.01)^2 + (0.01)^2} = 0.0141 = 1.41\,\% \tag{3.2}$$

For the measurement of the temperature of the DC/DC converter, a CAN BOX was used. The thermal sensor was placed upon the thermistor on the PCB.

3.5.2 Battery module testing

The battery module consists of three individual batteries consisting of four Lithium NMC (Nickel Manganese Cobalt Oxide) cells with a cell voltage between $3-4.2$ V. The printed circuit board (PCB) with the DC/DC converter was connected directly to the cells.

Halogen bulbs of 12 V, 55 W were connected as a load and they were mounted on a plastic board with switches, see Figure 3.7a. These switches were able to be switched manually or via the terminal of the code debugger. There were six columns of lights making it to 24 lights in total. When switching on or off the lights the voltage quality could be studied and the behaviour of the DC/DC converters. The schematics for the system is displayed in Figure 3.7b. A capacitor was added in parallel with the load to simulate a more realistic impedance profile to mimic that of a car. The size of the capacitor was 10 mF and 16.6 mF.

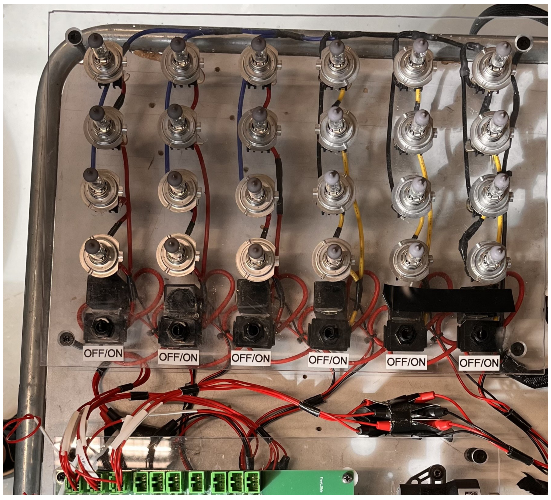

(a) Light switching board with connections to masterboard

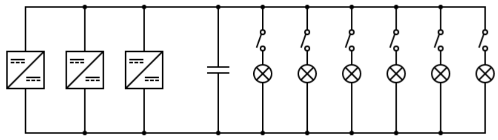

(b) Circuit diagram of the test setup with three DC/DCs

Figure 3.7: Switching board and schematic

The control system that was developed in PLECS was implemented in the hardware, i.e. the code where the DC/DC converter would shut itself down if the voltage on the secondary side was above its set voltage. Three DC/DC converters were then connected in parallel. The first DC/DC converter, DC/DC1, was set to a set voltage of 14.5 V whereas the other, DC/DC2, had a set voltage of 14.0 V and the third 13.5 V. A test sequence was performed where all six rows of lights were switched on and then off. The same test sequence was repeated for different gaps in set voltage between the DC/DC converters.

In Table 3.3 the test sequences performed are shown. The number of DC/DC converters activated and their set voltage can be seen, as well as the load switching pattern of the lights and the capacitance (see Figure 3.7). The test sequence is presented as a sequence of numbers where +X mean the turning on of X number of lamps and -X turning off. Each next step of the sequence is performed after one another according to a Python script.

Table 3.3: Testing sequences with specifications

DC/DCs	Set voltage [V]	Test sequence	Capacitance
1	14.5	4+2+2+2-6+6-2-2-2	10 mF
3	[14.5, 14.5, 14.5]	8+4+4+4+4-12+12-4-4-4-4	16.6 mF
3	[14.5, 14.0, 13.5]	4+4+4+4+4+4-12+12-4-4-4-4-4	16.6 mF

3.5.3 Software implementations

The DC/DC converter prototype had some protection implemented in the software, such as for over-current, voltage and heating. The DC/DC converter would turn itself off when the maximum limits for these values were reached. However, since all of these signals were oscillating, the DC/DC converter alternated between turning on and off. The temperature especially had this issue. Therefore, a hysteresis function was implemented where the DC/DC converter would turn off when it hit maximum temperature and also stay turned off until it cooled down to a normal operating temperature.

Just like in the PLECS model, a function for turning the DC/DC converter off when the output voltage was higher than its set voltage was done. Some margin had to be used here as well due to the ripple, meaning that the DC/DC converter should not be turned of as soon as the output voltage rose to about the set voltage, but when it rose above the set voltage plus an offset. The offset value was deemed to be okay at 0.5 V to not be disturbed by the ripple of ±0.2 V.

A function for overshoot of voltage when fast changes are made on the output was also implemented, allowing the DC/DC converter to go above the safety margin for a short period of time, depending on how long and how big the overshoot is.

When the DC/DC converter turns on or when there is a significant change in output voltage, there will be a high inrush current. Since the DC/DC converter needs to handle changes very fast, this current can not be limited but the DC/DC converter still needs protection from overcurrents. A software function was implemented to act like a definite time-overcurrent (DTOC) relay, allowing the current to go above the maximum value for a short period of time (1ms) and also a lower value for a longer period of time. This function separates the overcurrent for fast changes and fault currents, as a fault current will go on for a longer period of time resulting in turning off the DC/DC converter before any damage is done to itself and the external circuit.

The function for warning the system that a large load change is inbound and changing the set voltage of the DC/DC converters was not able to be implemented into the hardware.

4

Results and analysis

The results and analysis from the PLECS simulation and the hardware testing are presented in this chapter.

4.1 Load switching sequences

Below follows plots comparing the hardware and PLECS model. All tests were performed on the battery module with the light switching board connected (as in Figure 3.7), stepping up and down in load according to Table 3.3. The same load sequence was simulated in PLECS.

4.1.1 One DC/DC converter

The sequence where the load of light bulbs were switched on and off was replicated in PLECS as well for comparison. The sequence of switching on four loads every 0.2 seconds is shown in Figure 4.1 for a single DC/DC converter for both the PLECS model (4.1a) and the hardware with and without capacitor (4.1b and 4.1c). The PLECS model had no capacitor connected to the circuit.

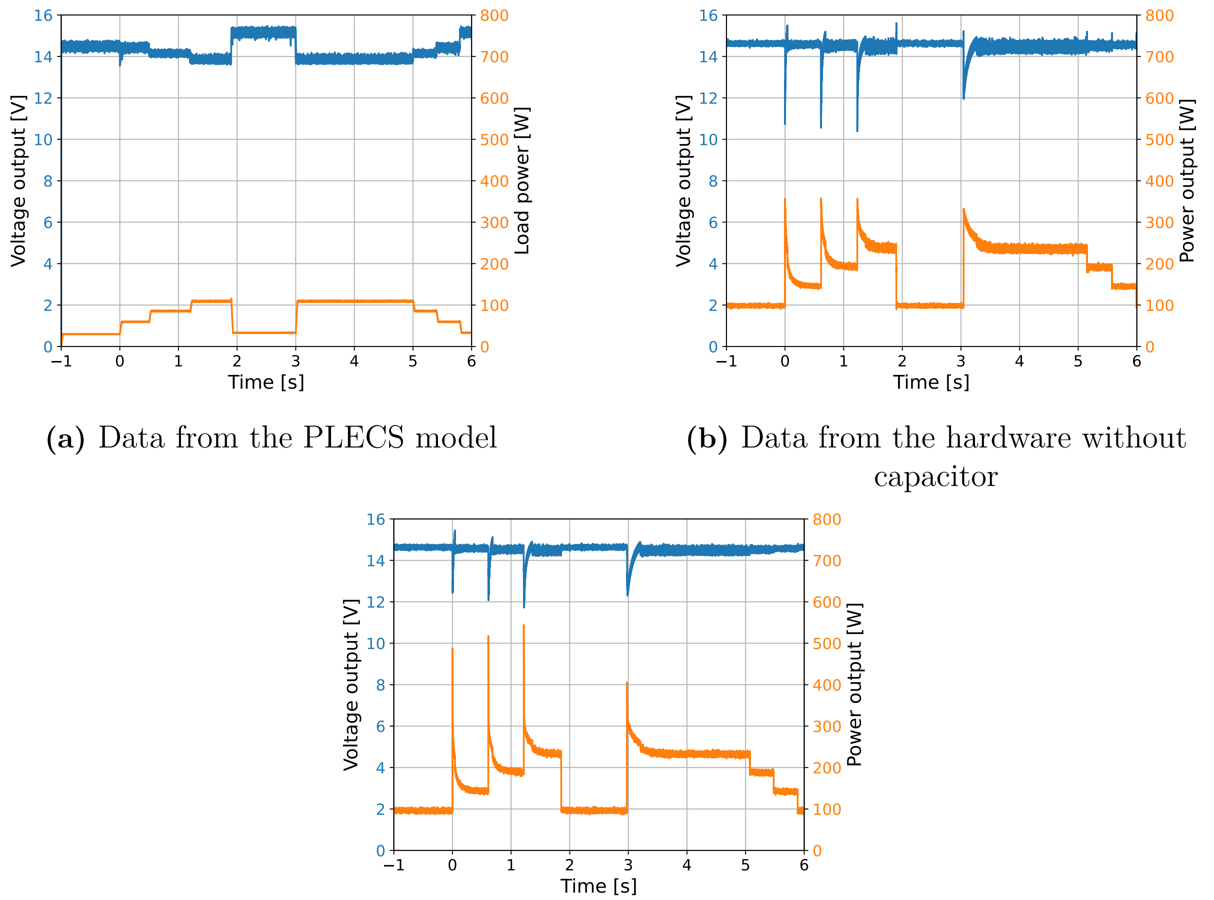

(a) Data from the PLECS model

(b) Data from the hardware without capacitor

(c) Data from the hardware with capacitor

Figure 4.1: Increasing the load of a system of one DC/DC at set voltage 14.5 V. The output voltage is plotted in blue and the output power in orange

The DC/DC was capable of maintaining an output voltage within the specified limits of $9 - 16$ V with the set voltage of 14.5 V. The higher the load, the greater the voltage drop will be but it is not increasing proportionally to the load. The voltage is noisier at higher loads and there is also a clear improvement with the use of a capacitor, as was expected.

The PLECS model does not represent the hardware when it comes to the voltage drops that occur at the moment of an increase in electrical load.

The response time of the system has also been studied for each case, below in Figure 4.2 the output voltage has been zoomed in on and response time has been calculated.

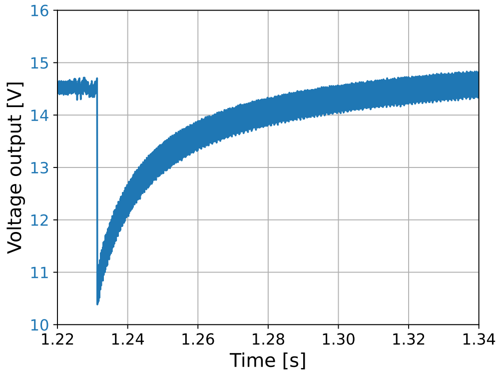

(a) Without a capaictor

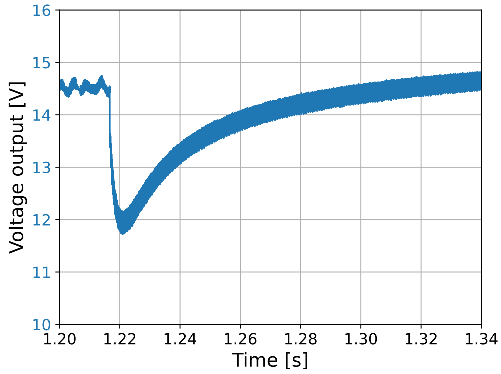

(b) With a capacitor

Figure 4.2: Response time for 1 DC/DC converter at a step of the load increasing

The fall time for the case without a capacitor, the voltage drop is almost instant with a fall time of 0.150 ms which is not acceptable for the LV124 standard. The fall time, as expected is improved with a capacitor, increasing the fall time to 4.09 ms. However, this is still below the requirement of 300 ms. The rise time for both cases is acceptable as they are both below the requirement of maximum 300 ms.

The rise and fall time (t_r and t_f) are presented in Table 4.1.

Table 4.1: Rise and fall time for Figure 4.2

	t_f [ms]	t_r [ms]
Without capacitor	0.150	106.2
With capacitor	4.09	88.13

4.1.2 Multiple DC/DC converters

The same sequence is shown in Figure 4.3 but for three DC/DC converters. The load at each step has been increased and the DC/DC converters are all set to the same set voltage, 14.5 V.

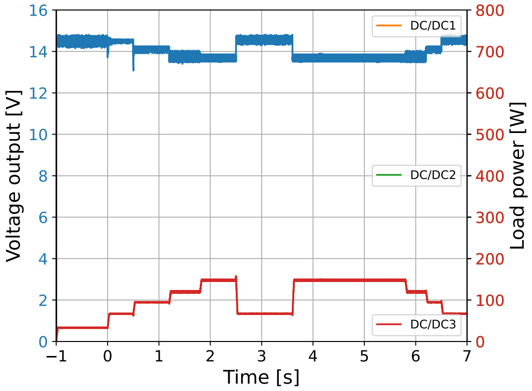

(a) Data from the PLECS model

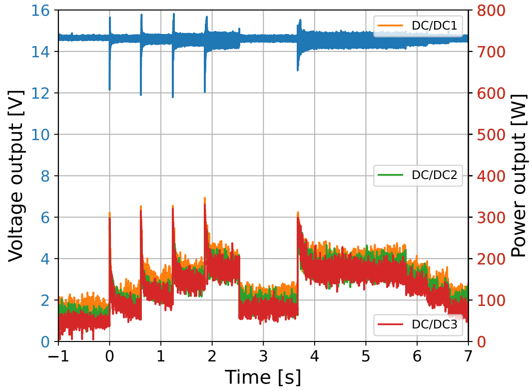

(b) Data from the hardware without a capacitor

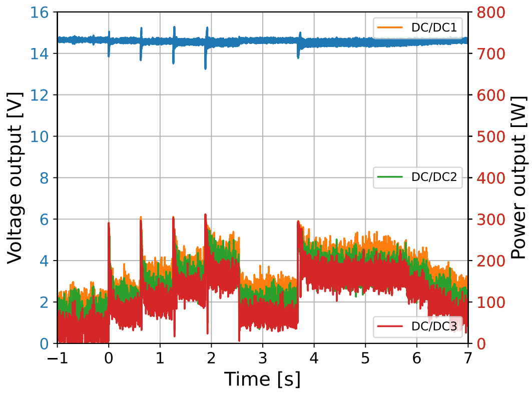

(c) Data from the hardware with a capacitor

Figure 4.3: Increasing the load of a system of three DC/DC converters all set at 14.5 V. The output voltage is plotted in blue and the output power from each DC/DC converters is plotted in orange, green and red

As with one DC/DC converter, the output voltage remains within the limits of $9-16\,\mathrm{V}$ as desired. The PLECS model is not presenting any large voltage drops or power transients as the hardware is. However, the steps in output voltage in the PLECS model are more distinguished than in the hardware. The hardware output voltage does not decrease as much as the PLECS model, nevertheless the output voltage from the hardware becomes increasingly noisier as the load increases.

Below in Figure 4.4 the output voltage has been zoom in on and the response time has been calculated.

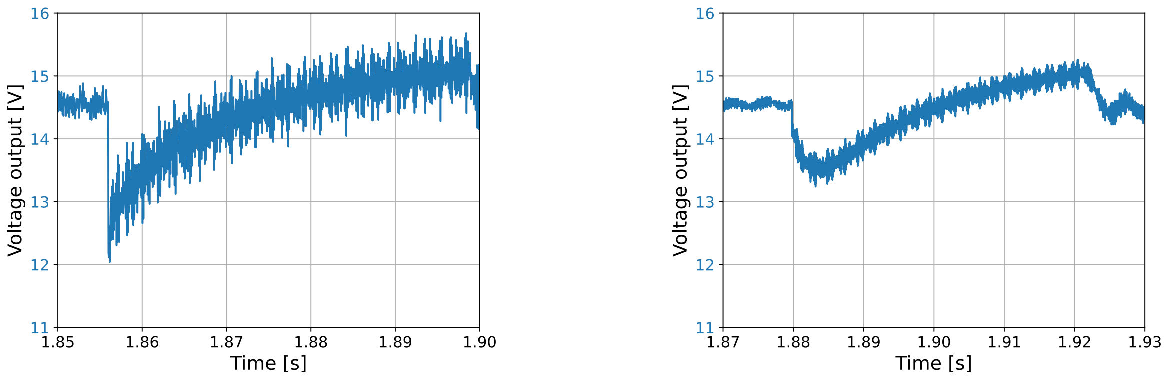

(a) Without a capacitor

(b) With a capacitor

Figure 4.4: Response time for 3 DC/DC converters at the same set voltage at a step of the load increasing

The rise and fall time (t_r and t_f) are presented in Table 4.2.

Table 4.2: Rise and fall time for Figure 4.4

	t_f [ms]	t_r [ms]
Without capacitor	0.198	23.3
With capacitor	3.38	16.54

Figure 4.5 shows the three DC/DC converters at different set voltages.

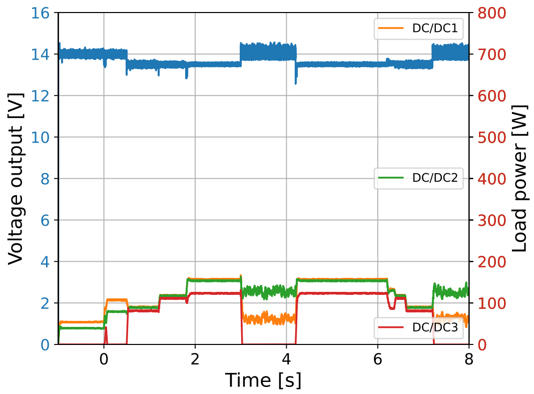

(a) Data from the PLECS model

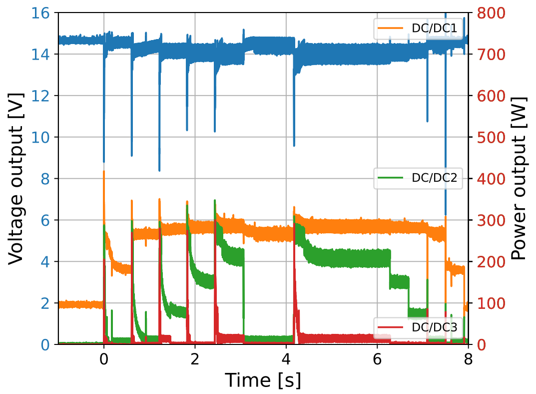

(b) Data from the hardware

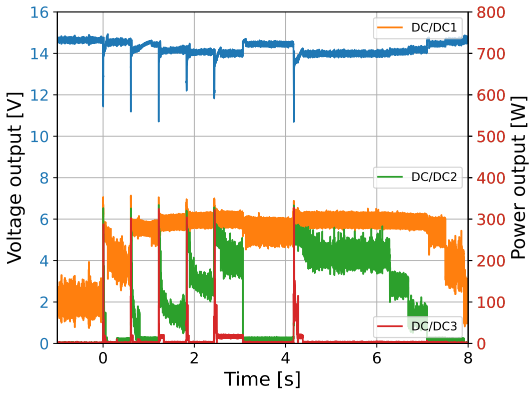

(c) Data from the hardware with a capacitor

Figure 4.5: Increasing the load of a system of three DC/DC converters. DC/DC1 has a set voltage of 14.5 V, DC/DC2 has 14.0 V and DC/DC3 has 13.5 V. The output voltage is plotted in blue and the output power from each DC/DC converter is plotted in orange, green and red

The three DC/DC converters were set on different set voltages, thus only the highest one operating at low load levels. Unlike from the previous test setups, this case does not fulfil the LV124 requirement without the capacitor, as can be seen in Figure 4.5b. It is only with a capacitor of 16.6 mF that the output voltage stays within $9 - 16$ V.

Below in Figure 4.6 the output voltage has been zoom in on and the response time has been calculated.

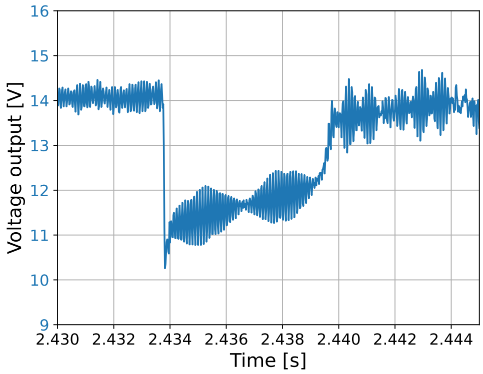

(a) Without a capacitor

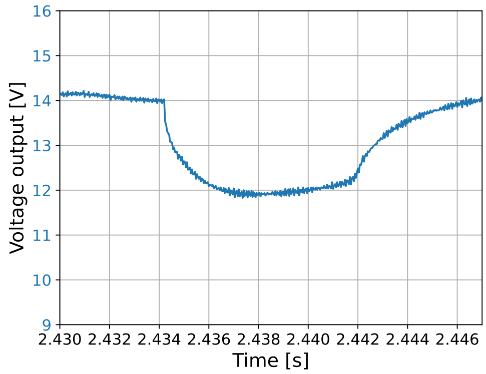

(b) With a capacitor

Figure 4.6: Response time for 3 DC/DC converters at different set voltages at a step of the load increasing

The rise and fall time (t_r and t_f) are presented in Table 4.3.

Table 4.3: Rise and fall time for Figure 4.4

	t_f [ms]	t_r [ms]
Without capacitor	0.200	6.5
With capacitor	2.8	7.25

When the load is changed, the output voltage is dropped and the secondary DC/DC converter in the set voltage list starts to boost the output voltage and turns off as the first one can keep the voltage stable. When the next load change has occurred the second one keeps going to keep the voltage stable at the second set voltage. The voltage drop becomes smaller when two DC/DC converters are operating at the time even though the load is higher, the change in load is still the same for each step. Since two DC/DC converters are capable of handling the load at the second set voltage, the third DC/DC converter is only active when the load increase for a very brief moment.

It is clear that the voltage stability is better for the test case when all the converters are at the same set voltage. A reason for this could be that when a load is switched on, the DC/DC converters that are active need to regulate themselves and increase the power output. If three converters are active, they all regulate at the same time and they split the power load. If only one DC/DC converter is active, that converter needs to regulate alone at first, until the output voltage drops to the level of the next converter's set voltage and then that one kicks in and starts helping. This could be an explanation to why the voltage drops are deeper for the case with different set voltages. Still, even though the output voltage was not as stable for the case with different set voltages, it still fulfils the LV124 requirement when the capacitor is connected to the circuit.

The response time of the system was also studied for same set voltage and different set voltages, with and without capacitor. The fall time when switching on a load for both with and without capacitor is below the requirement of the LV124 standard (minimum fall time of 300 ms). There was no noticeable difference in fall time between operating with all DC/DC converters on same set voltage or on different set voltages. The rise time for the two different control strategies was in the acceptable level of the LV124 requirement of below 300 ms. When the DC/DC converters were working on different set voltages, the rise time was improved compared to the case with the DC/DC converters working at the same set voltage. This can be due to the larger voltage drops when operating at different set voltages, thus the DC/DC converters' PID-regulator have to regulate a larger offset which results in a faster response time. It also needs to be taken into account that this test system does not represent all the loads in the vehicle, which can alter the dynamical behaviour of the voltage.

4.2 Overheating function

Due to the issue with overheating of the DC/DC converter, a hysteresis function for the temperature was implemented. When the temperature of the DC/DC converter was too high, the DC/DC converter should turn itself off and stay inactive until it has cooled down. Figure 4.7 shows such sequence, as well as the turning on of another DC/DC converter. There is a difference between the measured temperature and the temperature monitored by the DC/DC converter. This may be due to the possible misplacement of the temperature sensor and/or a faulty conversion from the DC/DC converter's temperature monitor. The maximum temperature of the DC/DC converter was set to 70 °C. The DC/DC converter itself, measured a temperature of 70 °C when it turned off, but as can be seen in Figure 4.7, the measured temperature only reached 58 °C.

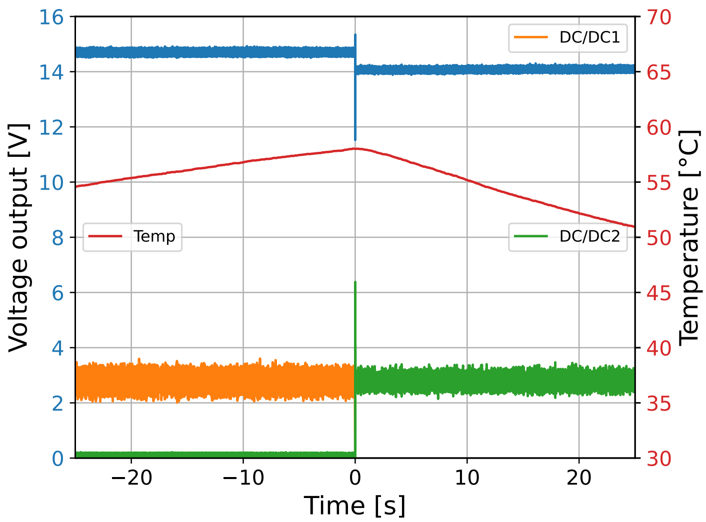

Figure 4.7: Overheating sequence with two DC/DC converters

The two DC/DC converters were set on two different set voltages, DC/DC1 having the highest set voltage. When DC/DC1 overheats and shuts down, DC/DC2 will increase its output to keep the voltage at its set voltage, thus there is a voltage drop before DC/DC2 takes over.

4.3 Multiple DC/DC converters handling WLTP cycle

Three DC/DC converters were connected in parallel and results from the simulation of a WLTP cycle can be seen in Figure 4.8. Maintaining a steady voltage output is of upmost importance, the output voltage of the PLECS model is therefore compared with that of an actual car in subfigure 4.8a. The profile for the load is shown in subfigure 4.8b and subfigure 4.8c shows the power output from each DC/DC. The distributed set voltages for the DC/DC converters in the PLECS model were 15.5, 14.5 and 13.5 V.

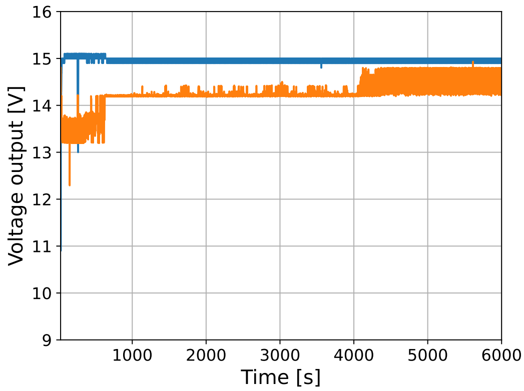

(a) Voltage output during a WLTP cycle comparing the PLECS model (orange) with that of an actual car (blue)

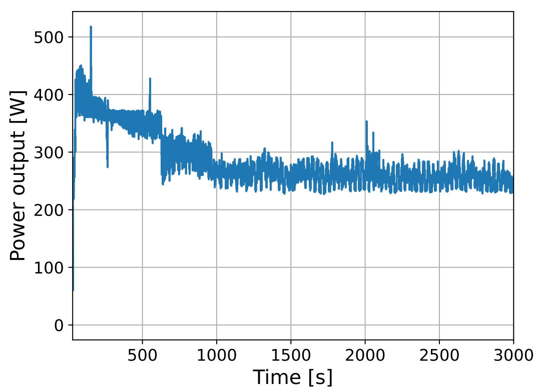

(b) The load profile in watts during the cycle

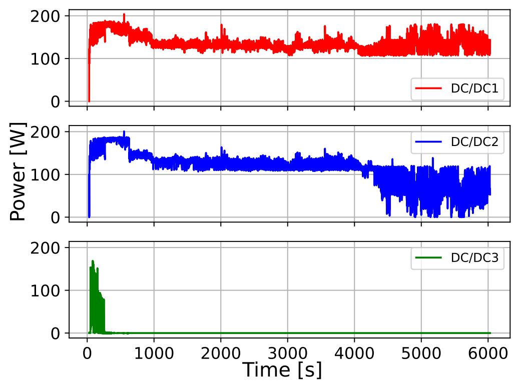

(c) The output power from each DC/DC during the cycle

Figure 4.8: Data from a WLTP cycle plugged into the PLECS model of the DC/DC converter system

It is clear that the output voltage from the PLECS model fulfils the LV124 requirement. However, as can be seen from section 4.1, the PLECS model does not model the large voltage drops that occur when switching on an additional electrical load.

The PLECS model has limited each DC/DC converter to only output roughly 200 W. It is clear that as soon as the converters hit their limit, the next converter kicks in. This can be seen in the beginning where the output power is above 400 W, which means that three DC/DC converters should be active. At the same time in the simulation the output voltage then had dropped to approximately 13.5 V, which is the set voltage of the third DC/DC converter. As can be seen, the output power never goes below 200 W, which leads to two DC/DC converters constantly being active during the simulation, which in turn leads to the output voltage never going above the set voltage of the second DC/DC converter, i.e. 14.5 V.

Large transient were added to the WLTP cycle to see how the system would handle that. Figure 4.9 shows the output voltage and power of the entire system as well as the output power for each DC/DC converter.

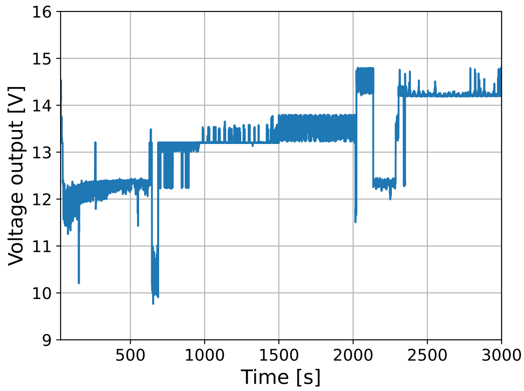

(a) Output voltage during the cycle

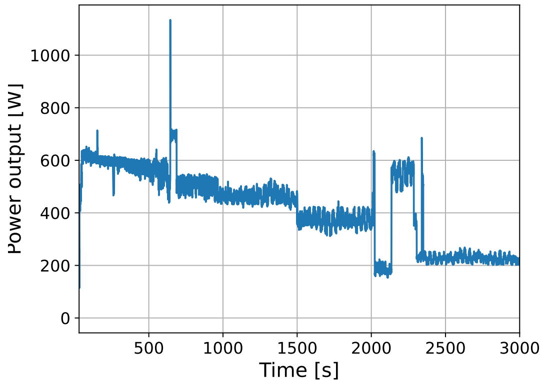

(b) Power output of the entire system during the cycle

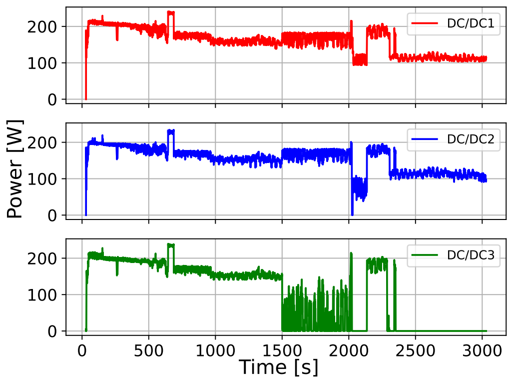

(c) Power output from each DC/DC during the cycle

Figure 4.9: Data from a WLTP cycle in PLECS with added transients in load

Since the maximum capacity of the three DC/DC converters should be 600 W it is expected that the output voltage should drop significantly for high load transients such as the ones well above 600. What is promising to see is that the DC/DC converters all react instantly and can supply power as soon as it needs. Even DC/DC3, which was turned off during a period of time in subfigure 4.9c turned on instantly when the output power was increased.

4.4 Efficiency

Efficiency measurements were performed on a single cluster board and are presented in Figure 4.10. Measurements were taken for three different input voltages 13, 14.5 and 16 (Figures 4.10a, 4.10b and 4.10c respectively). For each input voltage the set voltage and load was varied.

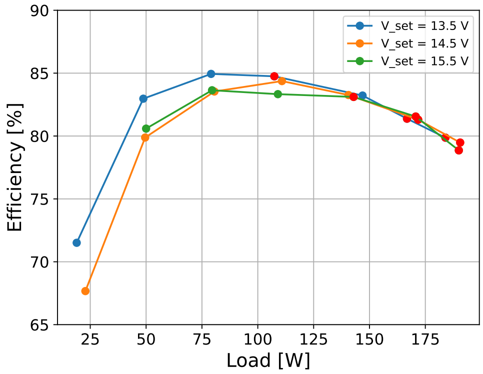

(a) Input voltage 13 V

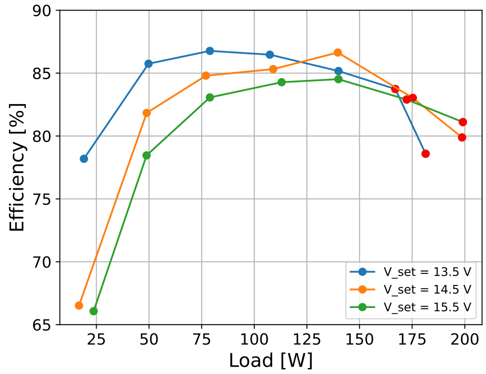

(b) Input voltage 14.5 V

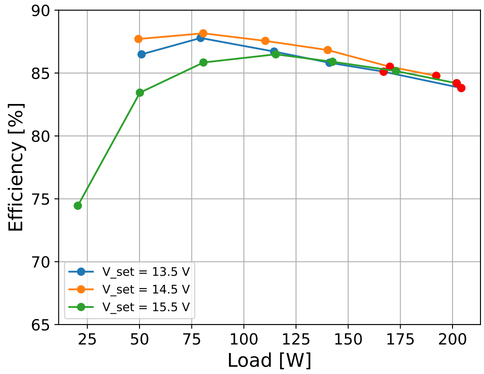

(c) Input voltage 16 V

Figure 4.10: Efficiency plots for different set and input voltages. Data points marked as red dots are where the DC/DC converter could no longer hold the desired output voltage. The blue line shows the efficiency depending on the load for set voltage equal to 13.5, orange line for 14.5 and green line for 15.5

The hardware was supposed to be able to produce 200 W maximum, but as seen in Figure 4.10 the efficiency is significantly lower for higher loads and the DC/DC converter was not able to maintain the set voltage. Measurements for all too low loads were not able to be done either. The lowest load that the DC/DC converter could handle depended on the gain. Going from a higher input voltage, 16 V to a lower output voltage, 13.5 or 14.5 V, limited the converter to the lowest load of approximately 50 W. For all other combinations of input voltage and output voltage the lowest load was around 20 W.

There are multiple reasons for this limited behaviour in the hardware. Firstly, there could be some technical design problem. Moreover, the DC/DC converter was not running in its designed environment. There was no cooling applied to the DC/DC converter. The power supply is not representing the battery properly because the power supply uses switches to convert the AC voltage input to a DC output voltage. A battery reacts faster than the power supply since it can apply the DC voltage directly. The programmable electronic load is only resistive while the load in the vehicle can be resistive, inductive and capacitive.

Simulating one DC/DC converter in PLECS gave the following efficiency results in Figure 4.11.

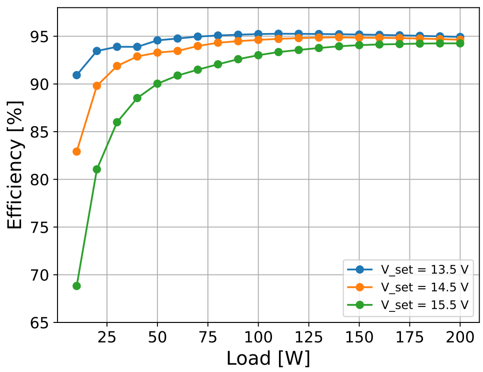

(a) Input voltage 13 V

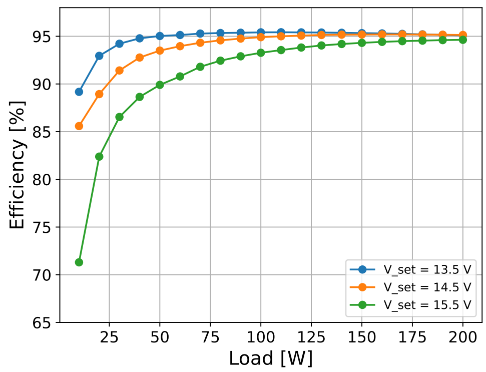

(b) Input voltage 14.5 V

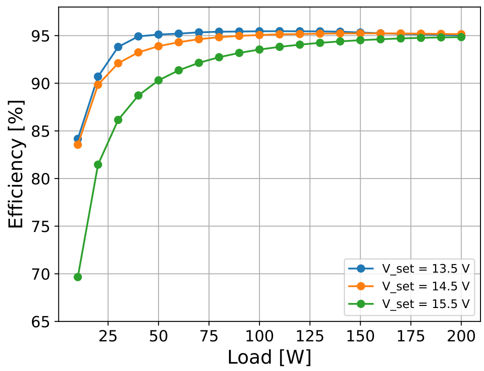

(c) Input voltage 16 V

Figure 4.11: PLECS efficiency plots for different set and input voltages. The blue line represents a set voltage of 13.5 V, the orange lines 14.5 V and the green lines 15.5 V

Overall, the efficiency in PLECS, even with switching and core losses included, is higher than what was determined from the hardware. However, the overall behaviour of the efficiency depending on loads, input and output voltage are expected. Generally, the efficiency was better for higher loads and there is a small increase in efficiency for higher input voltages evident in Figure 4.11.

Since regular driving usually consumes $20 - 30$ A, and with the goal to deliver 15.5 V, the optimal system would be to have as few DC/DC converters on as possible. As can be seen in Figure 4.11, the efficiency during low loads are best for a lower set voltage. This is good since the idea for the control of a system of DC/DC was to have the majority of the DC/DC converters activated at 13.5 V, which leads to the load being split over a larger number i.e. lower load for one single DC/DC.

The losses that were included in the simulations were the conduction and switching losses of the MOSFETs on the primary side as well as the winding and core losses of the transformer. Figure 4.12 presents the average of these losses for a sweep of different loads for the DC/DC converter. Only one case is plotted, where the input voltage is 16 V and the output voltage is 15.5 V. For all the different cases, the behaviour of the losses were the same but a slightly changed value.

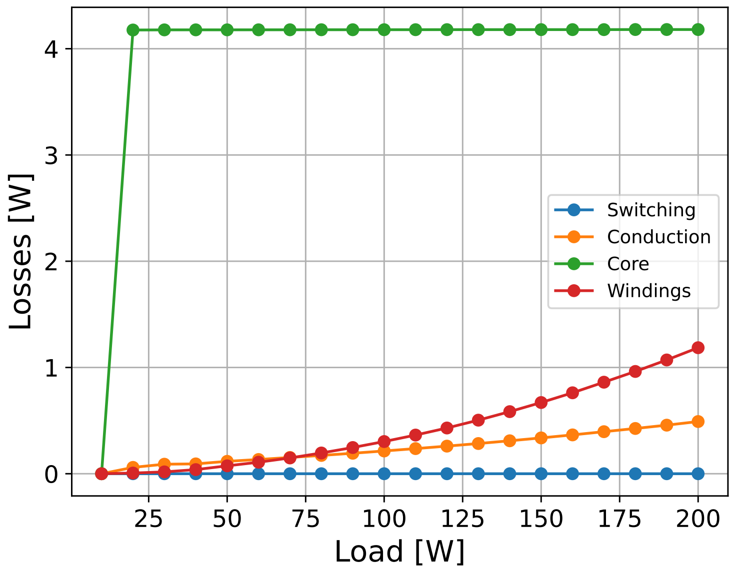

Figure 4.12: Losses plotted while sweeping over the load

The core loss is by far the largest factor and was calculated using Steinmetz's equation (2.7). This can be realistic as the highest source of heat for the hardware was from the transformer, indicating that this was where a lot of the losses were. The other losses are very low in comparison, the switching losses seem to be zero but they are of the order 10^{-7}. This may not correspond to the hardware as the losses for the hardware are of a greater factor.

4.4.1 Test sequence

The efficiency measurements from the three different test sequences from Table 3.3 are shown in Figure 4.13.

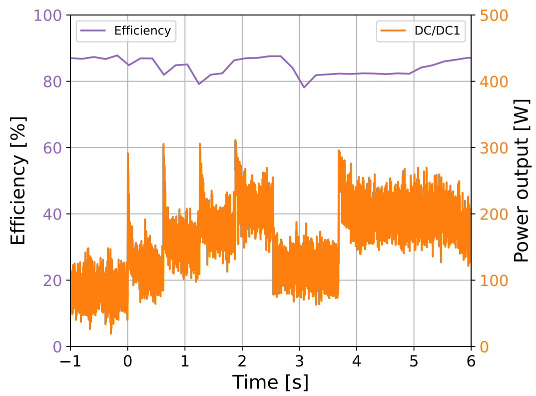

(a) One DC/DC active

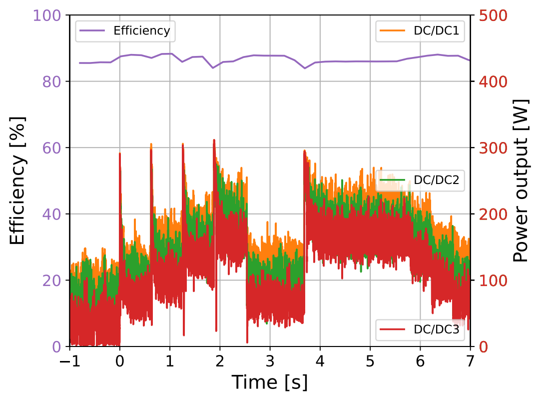

(b) Three DC/DC converters with the same set voltage

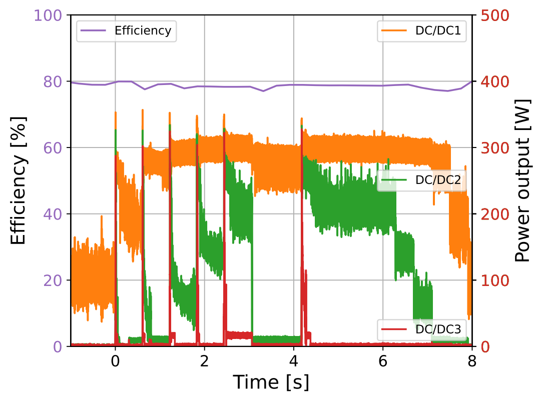

(c) Three DC/DC converters with different set voltages

Figure 4.13: Test sequence plots showing the efficiency during the cycle

Table 4.4 summarized the efficiency ranges for the three different test cases above in Figure 4.13.

Table 4.4: Efficiency for three test sequences

DC/DC converters	Set voltage [V]	Efficiency [%]	Average Efficiency [%]
1	14.5	77.1 – 87.8	84.01
3	[14.5, 14.5, 14.5]	83.9 – 88.3	86.66
3	[14.5, 14.0, 13.5]	77.0 – 80.6	78.56

From Figure 4.13 and Table 4.4 it is clear that the efficiency during the test sequence was better in the setup with the DC/DC converters operating at the same set voltage, contrary to what was theoretically hypothesized. This may however have to do with the hardware design. As was seen from Figure 4.10 the DC/DC converter does not have an increased efficiency for higher loads as it is supposed to be for the LLC resonant converter. Should it have operated as in theory, without any possible design faults, the efficiency curve would probably look more similar to the simulated ones in Figure 4.11. This would more likely have resulted in a different result in efficiency during the different test setups from Table 4.4.

5 Conclusion

The system was able to operate within the limits of the LV124 standard when increasing and decreasing the load for all cases with a capacitor added to the system. The system fulfilled the requirement even without a capacitor for each of the cases besides the one with different set voltages. Since the load was only resistive, adding a capacitor parallel with the load to help with maintaining the voltage at switching point, the voltage stability was improved.

The voltage drop at the switching point was decreased when several DC/DC converters were operating at the same set voltage. Therefore, the initial idea of having 2-3 DC/DC converters at the top of the control hierarchy might need to be adjusted. The voltage stability of the system would handle an electrical load transient better if there were more DC/DC converters active. Hence the control hierarchy might need to be further analysed and matched with a WLPT cycle to see how many DC/DC converters need to be set at 15.5 V for basic driving to avoid large voltage drops.

When the DC/DC converters are operating at different set voltages, the load will not be split evenly between them. This can cause one of the DC/DC converters to be working at high load and another one at low load, which causes instability since a low load operating point for the DC/DC converter is not optimal. When one of the DC/DC converter is working at the maximum operating point, it will cause ripple in the voltage which turns on the next DC/DC converter in the voltage hierarchy. The DC/DC converter on a lower set voltage will then go on and off, which causes disruption to the system. The unevenly distribution of the load will also stress one of the DC/DC converters more than the others, e.g. the temperature will rise quicker in the one working harder. This is of course an issue since too high temperature causes wear on the electric components.

The function for changing the set voltage of the converters before a planned load change was not able to be conducted. However, comparing the voltage drops between the two cases when the converters are operating at the same voltage level and the other case, operating on different levels, it can be concluded that a change in set voltages before planned load step happens will have an improvement on voltage stability. Therefore, the conclusion can be drawn that this software function is recommended to be implemented in future work.

As was seen, the voltage stability in PLECS did not show similar behaviour when it comes to voltage drops in the hardware. It was expected that the simulated model would not represent the hardware perfectly since they depend on different control strategies, among other things.

All in all, a system of three DC/DC converters can handle loads from $50 - 600\,\text{W}$ with acceptable voltage stability. The ripple was around $\pm 0.2\,\text{V}$ and the largest voltage drops where $2\,\text{V}$, which a car should be able to handle. The ripple and voltage drops were reduced with a capacitor connected in parallel with the load. The capacitors used were $16.6\,\text{mF}$ at the largest and were supposed to simulate a scaled capacitive environment of the car.

The results regarding efficiency for the system proved to be slightly better with the setup of three DC/DC converters at the same set voltage, compared to the setup with different set voltages. The efficiency ranged from $83.9 - 88.3\,\%$ for the setup with the same set voltage, whereas for the one with different set voltages it was $77.0 - 84.1\,\%$. Although, one conclusion from the hardware tests is that it is not designed optimally. The hardware does not follow the behaviour of an LLC resonant converter, which should increase in efficiency with increased loads, as simulated in Figure 4.11. Rather than increasing in efficiency, it decreases as well as not being able to maintain its set voltage. This is the main reason for the unexpected results regarding the test setup of different versus same set voltages of the DC/DC converters.

5.1 Future work

One of the future goals of this project is evidently to apply the MLC in a car. For that to work, a lot more than only three DC/DC will need to interact with each other. The issues we have encountered that would need to be fixed for this goal to be achieved are mainly the hardware issue and a solution to distribute the load evenly between the DC/DC converters.

Solving the load distribution problem could be done with the implementation of droop control. This could possibly reduce, or completely remove, the phenomenon of the DC/DC converters working against each other and make them distribute the load evenly [12]. The implementation of a droop control would however include additional feedback to and from the masterboard. Unfortunately, this introduces further vulnerability and the goal of the system is to be as robust as possible and rely on outside communication as little as possible. Another solution could be to change the set voltages of the DC/DC converters when operating. As it is right now, the DC/DC converters have their initial set voltage and when the output voltage drops below that, the DC/DC converters with a higher set voltage still try and regulate the voltage back up to their set voltage, causing them to work harder and outputting more power than the others. If the DC/DC converters with a higher set voltage than the output voltage had their set voltage changed to the lowest set voltage of the active DC/DC converters, then they should all be working equally.

Bibliography

[1] International Energy Agency. *Global EV Outlook 2023*. 2019. URL: https://www.iea.org/reports/electricity-information-overview/electricity-production (visited on 05/29/2024).

[2] International Energy Agency. *CO2 emissions intensity of electricity generation in the Announced Pledges Scenario, 2022-2030*. 2023. URL: https://www.iea.org/data-and-statistics/charts/co2-emissions-intensity-of-electricity-generation-in-the-announced-pledges-scenario-2022-2030 (visited on 05/29/2024).

[3] Oskar Josefsson. *Investigation of a Multilevel Inverter for Electric Vehicle Applications*. 2015. URL: https://publications.lib.chalmers.se/records/fulltext/214013/214013.pdf (visited on 05/13/2024).

[4] Hasaan Farooq et al. "Loss Analysis of Full Bridge LLC Resonant Converter with Wide Input Range Using Si and SiC Switches". In: *2021 16th International Conference on Emerging Technologies (ICET)*. 2021, pp. 1–6.

[5] Subhashish Bhattacharya Suyash Sushilkumar Shah Utkarsh Raheja. *Input Impedance Analyses of Charge Controlled and Frequency Controlled LLC Resonant Converter*. URL: https://www.freedm.ncsu.edu/wp-content/uploads/2018/10/ECCE-2018-Input-Impedance-Analyses-of-LLC-Resonant-Converter-Shah-Bhattacharya.pdf (visited on 05/13/2024).

[6] T. Hudson. *Understanding LLC Operation (Part I): Power Switches and Resonant Tank*. URL: https://www.monolithicpower.com/understanding-llc-operation-part-i-power-switches-and-resonant-tank (visited on 02/05/2024).

[7] H. Huang. *Designing an LLC Resonant Half-Bridge Power Converter*. Texas Instrument, 2010.

[8] Sam Abdel-Rahman. *Resonant LLC Converter: Operation and Design*. 2012. URL: https://www.infineon.com/dgdl/Application_Note_Resonant+LLC+Converter+Operation+and+Design_Infineon.pdf?fileId=db3a30433a047ba0013a4a60e3be64a1 (visited on 05/23/2024).

[9] T. Hudson. *Understanding LLC Operation (Part II): What to Consider in LLC Converter Design.* URL: https://www.monolithicpower.com/understanding-llc-operation-part-ii-what-to-consider-in-llc-converter-design (visited on 04/22/2024).

[10] Sheng-yang Yu. *Power Tips: Why Is Your LLC Resonant Converter Frequency Way, Way off.* 2015. URL: https://www.ti.com/lit/ta/ssztc48/ssztc48.pdf?ts=1708336271557&ref_url=https%253A%252F%252Fwww.ti.com%252Fdocument-viewer%252Flit%252Fhtml%252FSSZTC48 (visited on 03/17/2024).

[11] Muhammad H. Rashid. *Power Electronics Handbook, 4th Ed.* Butterworth-Heinemann. p. 573, 2017.

[12] et al Yu Tang. *Adaptive droop control strategy of parallel LLC converters.* 2023. URL: https://research.ebsco.com/linkprocessor/plink?id=f28c74bf-38ad-363c-9053-1f5d26c0eda3 (visited on 06/17/2024).